

Brain Tumor And CAD Through MRI By Using Wavelet Transform And Genetic Algorithm

¹Pradeep Kumar, ²Md. Imtiyaz Anwar

ECE Deptt. Vidya Vihar Institute of Technology, Maranga, Purnea, Bihar-854301, India

Email: ¹pra_deep_jec@yahoo.co.in, ²imtiyaz.ece@gmail.com

Abstract

A brain tumor is an intracranial solid neoplasm, a tumor (defined as an abnormal growth of cells) within the brain or the central spinal canal. Magnetic Resonance Imaging (MRI) is one of the best technologies currently being used for diagnosing brain tumor. Brain tumor is diagnosed at advanced stages with the help of the MRI image. In this task, radiology experts are likely to benefit from the support of Computer Aided Diagnosis (CAD) systems to build around robust classification processes. In this paper, a method that combines wavelet transform for segmentation and genetic algorithm is used to yield high diagnostic classification accuracy for a broad range of brain tumour pathologies.

Keywords: Brain Tumor, MRI, Wavelet Transform, Genetic Algorithm.

1. Introduction

Brain tumor is inherently serious and life-threatening because of its invasive and infiltrative character in the limited space of the intracranial cavity. However, brain tumors (even malignant ones) are not invariably fatal. Brain tumors or intracranial neoplasm can be cancerous (malignant) or non-cancerous (benign); however, the definitions of malignant or benign neoplasms differs from those commonly used in other types of cancerous or non-cancerous neoplasm in the body. Its threat level depends on the combination of factors like the type of tumor, its location, its size and its state of development. Because the brain is well protected by the skull, the early detection of a brain tumor only occurs when diagnostic tools are directed at the intracranial cavity. Usually detection occurs in advanced stages when the presence of the tumor has caused unexplained symptoms. Over the last 20 years, the overall incidence of cancer, including brain cancer, has increased by more than 10%, as reported in the National Cancer Institute statistics (NCIS), with an average annual percentage change of approximately 1%. 2-6 between 1973 and 1985, there has been a dramatic age-specific increase in the incidence of brain tumors.

Now days, MRI is the noninvasive and very much sensitive imaging test of the brain in routine clinical practice. Magnetic resonance imaging (MRI) is a noninvasive medical test that helps physicians diagnose and treat medical conditions. An MRI machine uses a powerful magnetic field to align the magnetization of some atomic nuclei in the body, and radio frequency fields to systematically alter the alignment of this magnetization. This causes the nuclei to produce a rotating magnetic field detectable by the scanner—and this information is recorded to construct an image of the scanned area of the body. Magnetic field gradients cause nuclei at different locations to rotate at different speeds. By using gradients in different directions 2D images or 3D volumes can be obtained in any arbitrary orientation. Brain MRI is the procedure of choice for most brain disorders. It provides clear images of the brainstem and posterior brain, which are difficult to view on a CT scan. It is also useful for the diagnosis of demyelinating disorders (disorders such as multiple sclerosis (MS) that cause destruction of the myelin sheath of the nerve).

Often, the most determinant step in this computer-based data analysis is data pre-processing. For this, we first use the Discrete Wavelet Transform (DWT) and a filtering process, together with data compression, for the decomposition of the spectra in terms of approximation and detail coefficients, in a change of representation of the spectra that entails minimum loss of relevant information. This decomposition by itself does not alleviate the high dimensionality of the data. For this reason, dimensionality reduction is implemented using Moving Window with Variance Analysis (MWVA) for feature selection and Principal Components Analysis (PCA) for feature extraction. The processed data are classified using Artificial Neural Networks (ANN) with Bayesian regularization. The proposed combination of methodologies is shown to yield high diagnostic classification accuracy for a broad range of brain tumour pathologies, some of which have seldom been analyzed in this setting.

This paper is organised as follows: in section 2, various types of brain tumor is explained with symptoms. Section 3 deals about MRI. Section 4 describes about methodology with results and conclusion is given in section 5.

2. Brain tumor

Brain tumors include all tumors inside the cranium or in the central spinal canal. They are created by an abnormal and uncontrolled cell division, normally either in the brain itself (neurons, glial cells (astrocytes, oligodendrocytes, ependymal cells, myelin-producing Schwann cells), lymphatic tissue, blood vessels), in the cranial nerves, in the brain envelopes (meninges), skull, pituitary and pineal gland, or spread from cancers primarily located in other organs (metastatic tumors).

Aside from exposure to vinyl chloride or ionizing radiation, there are no known environmental factors associated with brain tumors. Mutations and deletions of so-called tumor suppressor genes are thought to be the cause of some forms of brain tumors. Patients with various inherited diseases, such as Von Hippel-Lindau syndrome, multiple endocrine neoplasia, neurofibromatosis type 2 are at high risk of developing brain tumors. In a recent study by the Dutch GP Association, a list of causes of headaches was published, that should alert GP's to take their diagnosis further than to choose for symptomatic treatment of headaches with simple pain medication (note the occurrence of brain tumors as possible cause) :

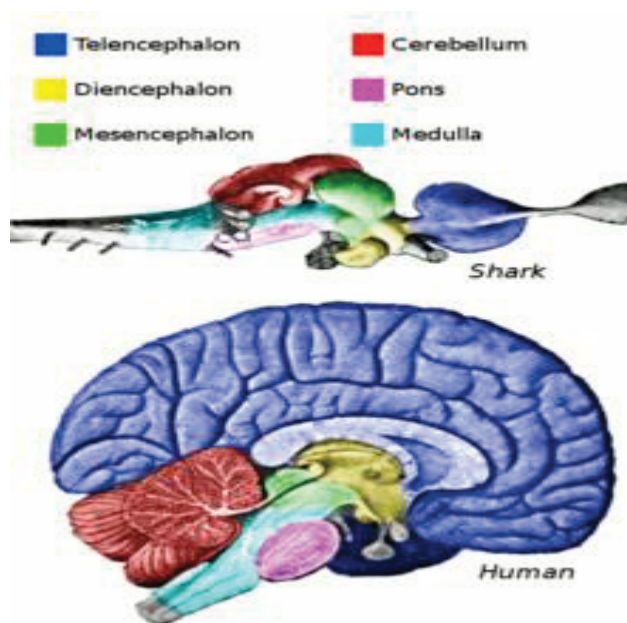


Fig:1. Main anatomical regions of the vertebrate brain

Table:1 Symptoms of brain tumor with causes

Alarm signals	Possible cause
First headache complaint from person over 50 years old	brain tumor, arteriitis temporalis
First migraine attack in person over 40 years old	brain tumor
Headache in person under 6 years old	brain tumor, hydrocephalus
Person over 50 years old with pain at temples	arteriitis temporalis
Pregnancy with unknown headache	pre-eclampsia
Increased headaches after trauma	sub/epidural hematoma
Severe headaches and very high blood pressure	malignant hypertension
Acute severe headache	meningitis, CVA (Cerebrovascular accident or stroke), subarachnoidalhemorrhage
Headache and fever (with reduced consciousness)	meningitis
Stiffness of the neck/neurological	meningitis, brain tumor

dysfunction	
Headache with signs of elevated intracranial pressure	brain tumor
Focal neurological dysfunction	brain tumor
Early morning vomiting or vomiting unrelated to headache or other illness	brain tumor
Behavioral changes or rapid decline in school results	brain tumor

The visibility of signs and symptoms of brain tumors mainly depends on two factors: tumor size (volume) and tumor location. The moment that symptoms will become apparent, either to the person or people around him (symptom onset) is an important milestone in the course of the diagnosis and treatment of the tumor. The symptom onset - in the timeline of the development of the neoplasm - depends in many cases on the nature of the tumor but in many cases is also related to the change of the neoplasm from "benign" (*i.e.* slow-growing/late symptom onset) to more malignant (fast growing/early symptom onset). Symptoms of solid neoplasms of the brain (primary brain tumors and secondary tumors alike) can be divided in 3 main categories :

- Consequences of intracranial hypertension
- Dysfunction
- Irritation

3. Magnetic Resonance Imaging

Magnetic resonance imaging (MRI), nuclear magnetic resonance imaging (NMRI), or magnetic resonance tomography (MRT) is a medical imaging technique used in radiology to visualize detailed internal structures. MRI makes use of the property of nuclear magnetic resonance (NMR) to image nuclei of atoms inside the body. MRI provides good contrast between the different soft tissues of the body, which makes it especially useful in imaging the brain, muscles, the heart, and cancers compared with other medical imaging techniques such as computed tomography (CT) or X-rays. Unlike CT scans or traditional X-rays, MRI does not use ionizing radiation.

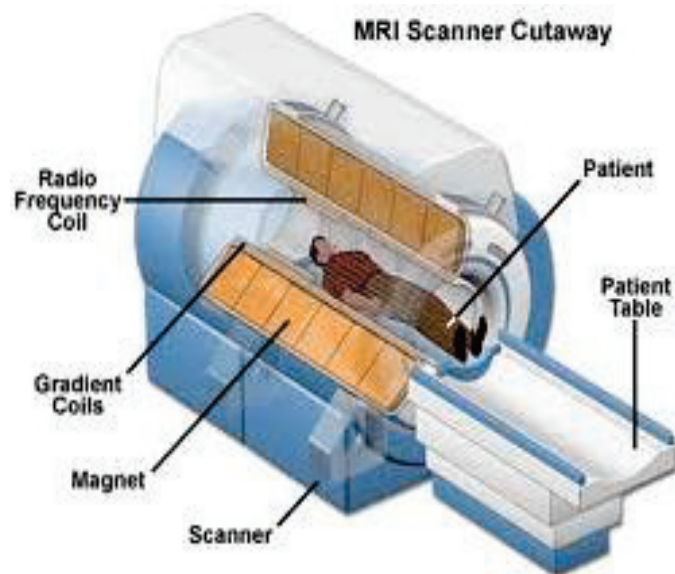


Fig.2. Cutaway of MRI scanner

A number of features of MRI scanning can give rise to risks. These include:

- Powerful magnetic fields
- Cryogenic liquids
- Noise
- Claustrophobia

4. Methodology and Results

A. Wavelet Transform

The Wavelet Transform (WT) is a linear operation that decomposes a signal into components at different scales [4]. The WT of a function $f(t)$ for a wavelet function $\psi(t)$ is given by (1), where a is the scale and τ the position of the wavelet $\{a, \tau: \mathbb{R}\}$. The inverse transform is given by (2).

$$Wf(a, \tau) = \frac{1}{\sqrt{a}} \int_{-\infty}^{\infty} f(t) \psi\left(\frac{t-\tau}{a}\right) dt \quad (1)$$

$$f(t) = \frac{1}{K_{\psi}} \iint_{-\infty}^{\infty} Wf(a, \tau) \Psi(a, \tau) \frac{da d\tau}{a^2} \quad (2)$$

$$K_{\psi} = \int_{-\infty}^{\infty} \frac{|\Psi(w)|^2}{w} dw < \infty$$

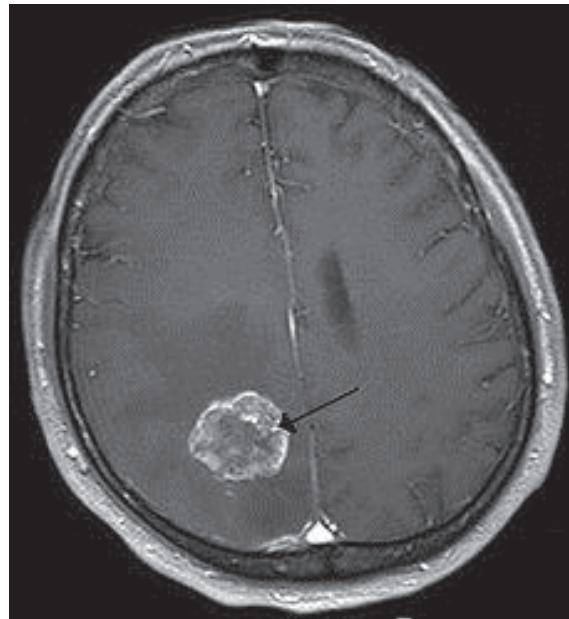


Fig:3. Brain metastasis in the right cerebral hemisphere after MRI

An important development for the application of wavelet theory in Discrete Signal Processing was presented by Mallat using Multiresolution Analysis (MA). In this context, the WT in a discrete domain is implemented via an octave filter bank, as a cascade of low- and high-pass filters, followed by sub-sampling as illustrated in fig.4. The reconstruction procedure, except for rounding errors, leads to the restoration of the original signal if no coefficient is altered.

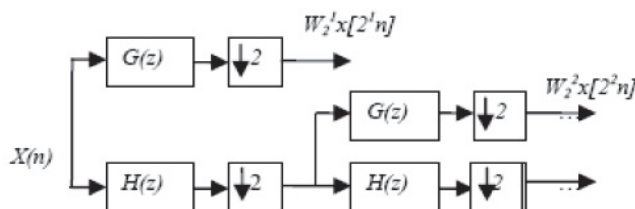


Fig:4. Decomposition algorithm of the DWT with two decomposition levels, the original signal $x(n)$ is passed through the high-pass filters $G(Z)$ and low-pass filters $H(Z)$.

The application of Mallat's model together with Donoho's approach for signal filtering by thresholding and statistical coefficients for data compression permit reducing the noise level, as well as representing the MRS signal without loss of relevant information, while keeping the dimensionality of the system as low as possible.

B. Wavelet Filtering with Threshold or Shrinkage

Frequently, the observed signal $X(t)$ can be considered to consist of a real signal $S(t)$ plus additive white noise $N(t)$. Shrinkage filtering aims to denoise the observed signal $X(t)$ and recover an estimate of $S(t)$, or $\hat{S}(t)$. The suggested model allows this through the use of WT as described in (3), where $D(.,\lambda)$ is the filtering operator for threshold λ and $W(\psi, j)(.)$ and $W^{-1}(\psi, j)(.)$ denote, in turn, the WT and its inverse, with wavelet function ψ and j decomposition levels. The denoising of the available MRS spectra was carried out according to the following three consecutive steps, each described in its own sub-section.

$$\begin{aligned}
 Y &= W_{(\psi,j)}(X) \\
 Z &= D(Y, \lambda) \\
 \hat{S} &= W_{(\psi,j)}^{-1}(Z)
 \end{aligned}
 \tag{3}$$

B.1. Threshold calculation

Three alternative choices of threshold were considered in the experiments, according to the following statistical estimators developed by Donoho:

- Universal threshold (Sqrtwolog): The threshold is chosen to be $\sqrt{2 \ln n}$, where n represents the length of the signal.
- Threshold applying the principle of Stein's Unbiased Risk (Rigrsure): The procedure requires obtaining a new vector $NV(k)$, rearranging data from minimum to maximum and taking the square root.
- Threshold Minimax: The threshold is selected following the minimax principle, commonly used in statistics to design estimators.

Sqrtwolog, Rigrsure and Minimax are function names taken from Matlab® wavelet toolbox.

B.2. Threshold scaling

The thresholds are usually weighted by a factor σ , a scaling of the mean absolute deviation based on the wavelet

decomposition level. Three types of weighting are considered:

- One: The weighting term is scalar (e.g., $\sigma = 1$).
- Sln: The weighting is computed by averaging the detail coefficients of the first level of decomposition, divided by 0.6745.
- Mln: As Sln but with the calculation of detail coefficients level by level.

B.3. Implementation of the threshold

Once the threshold is calculated and scaled, the thresholding process $D(Y, \lambda)$ is implemented through two alternative methods: Hard thresholding ($D_h(Y, \lambda)$) and Soft thresholding ($D_s(Y, \lambda)$) according to (4).

$$D_h(Y, \lambda) = \begin{cases} Y, & |Y| \geq \lambda \\ 0, & |Y| < \lambda \end{cases} \quad (4)$$

$$D_s(Y, \lambda) = \begin{cases} \text{sgn}(Y) (|Y| - \lambda), & |Y| \geq \lambda \\ 0, & |Y| < \lambda \end{cases}$$

C. Wavelet Mother Selection for MRS Data

The DWT was applied to the original signal data, making the decomposition to the maximum allowable level. It was implemented with different mother wavelets, ranging from different orders of Biorthogonals (1.1, 1.3, 1.5, 2.2, 2.4, 2.6, 2.8, 3.1, 3.3, 3.5, 3.7, 3.9, 4.4, 5.5, 6, 8), Coiflet (1 to 5), Daubechies (1 to 43), and Symlet (1 to 25). For every mother wavelet, the absolute values of each decomposition coefficient were sorted in descending order, and the signal of each spectrum was reconstructed by adding consecutive coefficients. The average Mean Square Error (MSE) and Signal-to-Noise Ratio (SNR) were calculated over the whole set of patients for each wavelet order r , together with the Number of Decomposition Coefficients (NDC). Finally, $Q1$ the index was computed as follows:

$$Q1(r) = \frac{\overline{SNR}_{Re}(r)}{\overline{MSE}_{Re}(r) + \overline{NDC}_{Re}(r)} \quad (5)$$

where r is the order analysed, and the Re sub index corresponds to the rescaled data between 1 and 3. The maximum values of $Q1$ indicate the orders with the best reconstruction error using the minimum NDC.

Once the initial set of wavelet orders were chosen, the filtering methodology explained in section B was used to denoise the spectrum signal and to eliminate irrelevant information. In order to determine the appropriated scaling, Donoho recommends the MSE as a measure of performance for each of the experiments. Therefore, the MSE was calculated for each spectrum of the reconstructed signal following the scheme described in (3), implementing all the options allowed by the combination of threshold estimation (Sqrtwolog, Rigrsure and Minimax), threshold scaling (Sln, One and Mln), and Hard thresholding. The Hard function was used because it

often yields smaller MSE than the Soft one, and also because it preserves the magnitudes of the MRS spectra. The results obtained show that, for all wavelets, the lower MSE is achieved when applying the Slnweighting scheme, regardless of the threshold calculation. The MSE of the three types of thresholds when Slnscaling is applied are compared in Fig.5, showing that the Rigsure-Sln-Hard procedure produces the best results among all combinations.

To determine the final wavelet, the average value of several statistics was computed for the Rigsure-Sln-Hard combination. They include: SNR, Preserved Energy (EP), Percentage of Distortion (PRD) and Compression Ratio (CR), expressed as follows:

$$EP = \frac{\sum_{k=1}^N [\hat{x}(k)]^2}{\sum_{k=1}^N [x(k)]^2} * 100 \quad (6)$$

$$PRD = \sqrt{\frac{\sum_{k=1}^N [x(k) - \hat{x}(k)]^2}{\sum_{k=1}^N [x(k)]^2}} * 100 \quad (7)$$

$$CR = L_o/L_c \quad (8)$$

where \hat{x} is the reconstructed signal, L_o is the cardinality of the decomposition coefficients of the original signal, and L_c is the cardinality of decomposition coefficients different to zero. This set of statistics has been used to choose the optimal wavelet in previous related works concerning ECG signal filtering and classification tasks, among others. For a more objective criterion in choosing the optimal wavelet function, the index $Q2$ was computed:

$$Q2(r) = \left[\frac{SNR_{Re}(r) + EP_{Re}(r) + CR_{Re}}{MSE_{Re}(r) + PRD_{Re}(r)} \right] \quad (9)$$

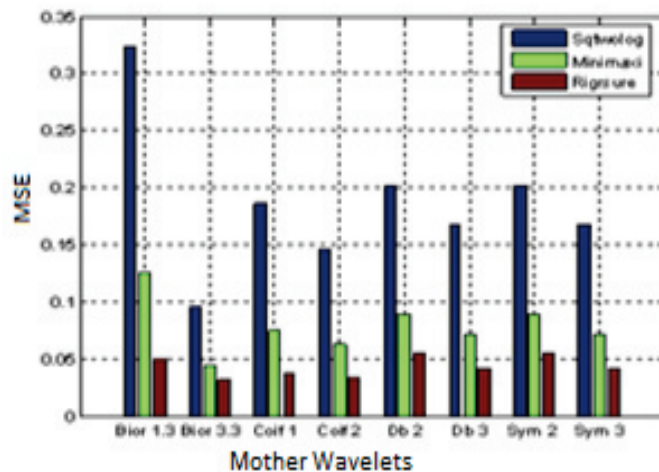


Fig:5. Comparison of the MSE for the three thresholds when Sln is applied.

The $Q2$ values for the wavelet functions. It can be observed that the maximum value for this index is given by the Biortogonal (3.3). Therefore, this wavelet was chosen as optimal for our study.

D. Dimensionality Reduction and Classification

After processing the MR spectra with wavelet Biortogonal (3.3) and filtering it with the combination Rigsure-Sln-Hard, we proceeded to reduce the dimensionality of the data using MWVA and PCA, taking as input variables the decomposition coefficients. The MWVA is a feature selection filter method proposed in. For PCA, principal

components were added one at a time until the differential cumulative variance between two consecutive components was less than 1%. An average of 10.15 and 13 variables were obtained for MWVA and PCA respectively.

Feed-forward ANN with one hidden layer were used in the classification experiments. Each network was trained using 5, 10, 30 and 40 units in the hidden layer and one unit in the output layer. The networks were trained with Bayesian regularization and back-propagation, updating the weights and bias according to the Levenberg-Marquardt algorithm. One run of a 5-fold cross-validation was performed for each network, with a maximum of 500 epochs. It shows the best resulting values of the area under the ROC curve (AUC) for each experiment. G1 (low grade gliomas) is the union of classes a2, oa and od. G2 (highgrade malignant tumours) is the union of classes gl and me. In this a value of 1 in the SET column indicates experiments which have been reported in previous research with, at best, comparable results, while a value of 2 indicates experiments that, to the best of our knowledge, have not been previously investigated in a similar setting.

The results of a Wilcoxon test show that the differences among the mean and median classification values for MWVA and PCA are statistically significant (p-value = 0.011), in favour of MWVA.

5. CONCLUSIONS

In this study, a DWT procedure was applied to the pre-processing of MR spectra corresponding to several brain tumour pathologies. This procedure yielded very encouraging results in terms of diagnostic discriminatory binary classification. In particular, they were quite good in the classification of pathologies for which few results, if any, had been previously reported. The results are of special relevance for the experiments gl vs me and a2 vs a3, which according to existing literature are specially difficult classification problems.

The proposed methodology for selecting the optimal wavelet developed study concludes that the Biortogonal (3.3) wavelet, implemented with the combination Rigsure-Sln- Hard, generates the best MR spectra representation without loss of relevant information.

ACKNOWLEDGMENT

The author would like to thank Dr. Abhay Kumar, Dr. Chanda Jha, for their insightful advice and guidance, and unknown reviewers for their useful remarks and suggestions.

REFERENCES

- [1] M. Murphy, A. Loosemore et al. "The contribution of proton magnetic resonance spectroscopy (1H MRS) to clinical brain tumour diagnosis", *Br J Neurosurg*, vol. 16, pp. 329–334, 2002.
- [2] M. Julià-Sapé, D. Acosta, M. Mier, C. Arús, D. Watson, and the INTERPRET Consortium, "A multi-centre, web-accessible and quality control checked database of in vivo MR spectra of brain tumour patients," *Magnetic Resonance Materials in Physics. MAGMA*, vol. 19, pp. 22–33, 2006.
- [3] C. Arizmendi, A. Vellido, E. Romero. "Frequency selection for the diagnostic characterization of human brain tumours", *Frontiers in Artificial Intelligence and Applications*, vol. 202, pp. 391-398, 2009.
- [4] P.D. Agoris et al. "Threshold selection for wavelet denoising of partial discharge data," *International Symposium on Electrical Insulation*, September 2004, USA.
- [5] S. Mallat, "A Wavelet Tour of Signal Processing," Academic Press, 1999, USA.
- [6] D. Donoho, "De-noising by soft-thresholding," *IEEE Trans. On Information theory*, vol.41, Issue. 3, pp. 613-627, 1995.
- [7] D. Guo -Fei et al. "A study of wavelet thresholding denoising," *IEEE Proceedings of ICSP*, vol.1, pp. 329-332, 2000.
- [8] O. Olarte, D. Sierra. "Determinación de los parámetros asociados al filtro wavelet por umbralización aplicado a filtrado de interferencias electrocardiográficas," *Universidad Industrial de Santander UIS Ingenierías*, vol. 6, Issue 2, pp 33-44, 2007.
- [9] E. Rivas, J. Burgos, J. García, "Condition assessment of power OLTC by vibration analysis using wavelet transform ". *IEEE Transactions On Power Delivery*, vol. 24, pp. 687-694, 2009.
- [10] F. Foresee, and M. T. Hagan. "Gauss-Newton approximation to Bayesian regularization," *Proceedings of the 1997 International Joint Conference on Neural Networks 1997*, pp. 1930-1935.

The IISTE is a pioneer in the Open-Access hosting service and academic event management. The aim of the firm is Accelerating Global Knowledge Sharing.

More information about the firm can be found on the homepage:
<http://www.iiste.org>

CALL FOR JOURNAL PAPERS

There are more than 30 peer-reviewed academic journals hosted under the hosting platform.

Prospective authors of journals can find the submission instruction on the following page: <http://www.iiste.org/journals/> All the journals articles are available online to the readers all over the world without financial, legal, or technical barriers other than those inseparable from gaining access to the internet itself. Paper version of the journals is also available upon request of readers and authors.

MORE RESOURCES

Book publication information: <http://www.iiste.org/book/>

Recent conferences: <http://www.iiste.org/conference/>

IISTE Knowledge Sharing Partners

EBSCO, Index Copernicus, Ulrich's Periodicals Directory, JournalTOCS, PKP Open Archives Harvester, Bielefeld Academic Search Engine, Elektronische Zeitschriftenbibliothek EZB, Open J-Gate, OCLC WorldCat, Universe Digital Library, NewJour, Google Scholar

